



EUROPEAN Geographical Studies

Issued since 2014
E-ISSN 2413-7197
2023. 10(1). Issued once a year

EDITORIAL BOARD

Rybak Oleg – Scientific Research Centre of the Russian Academy of Sciences, Sochi, Russian Federation (Editor-in-Chief)

Elizbarashvili Elizbar – Georgian Technical University, Tbilisi, Georgia (Deputy Editor-in-Chief)

Alexandrino Carlos – Institute of Science Engineering and Technology, Universidade Federal dos Vales do Jequitinhonha e Mucuri, Teófilo Otoni, Brazil

Abdrakhmatov Kanat – Institute of seismology NAS, Bishkek, Kyrgyzstan

Barmin Aleksandr – Astrakhan State University, Astrakhan, Russian Federation

Basilashvili Tsisana – Georgian Technical University, Tbilisi, Georgia

Chincharashvili Iza – Iakob Gogebashvili Telavi State University, Telavi, Georgia

Deene Shivakumar – Central University of Karnataka, Karnataka, India

Kalinichenko Valerii – Don State Agrarian University, Persianovsky, Russian Federation

Rajović Goran – Cherkas Global University, Washington, USA

Tikonov Vladimir – Lomonosov Moscow State University, Moscow, Russian Federation

Journal is indexed by: **CiteFactor** (USA), **CrossRef** (UK), **EBSCOhost Electronic Journals Service** (USA), **Electronic scientific library** (Russia), **Open Academic Journals Index** (USA), **Sherpa Romeo** (Spain), **Universal Impact Factor** (Australia).

All manuscripts are peer reviewed by experts in the respective field. Authors of the manuscripts bear responsibility for their content, credibility and reliability.

Editorial board doesn't expect the manuscripts' authors to always agree with its opinion.

Postal Address: 1717 N Street NW, Suite 1,
Washington, District of Columbia 20036

Release date 15.09.23.
Format 21 × 29,7/4.

Website: <https://egs.cherkasgu.press>
E-mail: office@cherkasgu.press

Headset Georgia.

Founder and Editor: Cherkas Global
University

Order № 120.

European Geographical Studies

2023

Is. 1

CONTENTS

Articles

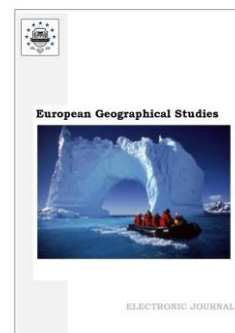
| | |
|--|----|
| Dangerous Weather Phenomena in Tbilisi and Associated Climate Risks E.Sh. Elizbarashvili, M.E. Elizbarashvili, Sh.E. Elizbarashvili | 3 |
| Statistical Characteristics of Hurricane Winds over Georgia for the Period 1961–2022 E.Sh. Elizbarashvili, O.Sh. Varazanashvili, A.G. Amiranashvili, S. Fuchs, T.Z. Basilashvili | 8 |
| Variations in the Tropopause Temperature and Height over the Vu Gia-Thu Bon River Basin in Vietnam: Insights from GNSS Radio Occultation Observations T. Hoai Thu Trinh, Q. Van Nguyen | 19 |

Copyright © 2023 by Cherkas Global University



Published in the USA
European Geographical Studies
Issued since 2013.
E-ISSN: 2413-7197
2023. 10(1): 3-7

DOI: 10.13187/egs.2023.1.3
<https://egs.cherkasgu.press>



Articles

Dangerous Weather Phenomena in Tbilisi and Associated Climate Risks

Elizbar Sh. Elizbarashvili ^{a, *}, Mariya E. Elizbarashvili ^b, Shalva E. Elizbarashvili ^a

^a Georgian Technical University, Institute of Hydrometeorology, Georgia

^b Ivane Javakhishvili Tbilisi State University, Georgia

Abstract

The probabilities of the occurrence of individual hazardous weather phenomena and their complexes in the city of Tbilisi were studied: hot days, strong winds, heavy winds, fog, hail, blizzard. The most common of the phenomena under consideration are hot days. Even in spring and autumn their probability is quite high, and in summer it reaches 0.83. During the cold season, there is a high probability of fog. Strong winds occur at all times of the year. Their probability is not very high, but is characterized by a significant coefficient of aggressiveness. Hail is especially aggressive and occurs in the warm season. The likelihood of a snowstorm developing is negligible.

Possible social and economic risks associated with these phenomena have been identified. Both social and economic risks are greatest from fog and strong winds. In winter, the economic risk from fog per incident can be more than 3.6 million US dollars, in the fall - more than 2.3 million US dollars. The social risk from strong winds is greatest in spring, although the risk is also significant in other seasons. The economic risk from strong winds in spring exceeds \$2.6 million, and in winter exceeds \$2 million. These phenomena occur several times throughout the year, so the economic risk can range from several to tens of millions of US dollars per year.

Keywords: dangerous phenomenon, probability, vulnerability, social and economic risk.

1. Introduction

Tbilisi is the capital of Georgia, the most important industrial, social and cultural center of the Caucasus, occupying a strategic position at the crossroads between Europe and Asia, which gives it the status of an important transit center for transnational energy and trade projects. The city is located in the Tbilisi Basin, stretching in a narrow strip for almost 30 km in the valley of the Kura River and along the mountain slopes adjacent on three sides. The height above sea level ranges from 380-770 meters. The area of the city is 726 sq. km. The population is 1,154,314 people (estimated for 2020). The climate is humid subtropical, with long hot summers, short warm springs and mild, but relatively dry winters.

Further development of the city requires a comprehensive account of its climatic features, especially dangerous weather phenomena, which often caused significant material damage to the

* Corresponding author

E-mail addresses: elizbar@hotmail.com (E.Sh. Elizbarashvili),
mariam.elizbarashvili@tsu.ge (M.E. Elizbarashvili), shalvaeliz@gmail.com (Sh.E. Elizbarashvili)

population (Elizbarashvili et al., 2013; Elizbarashvili et al., 2012; Elizbarashvili, Elizbarashvili, 2012; Varazanashvili et al., 2012). One of the authors of this article was an eyewitness to the catastrophic rainfall observed on June 7, 1972 in Tbilisi, when more than 100 mm of precipitation fell in a short period of time (245 minutes) (Elizbarashvili et al., 2020; Elizbarashvili et al., 2019). The downpour caused significant material damage to industrial enterprises, communications, transport, utilities and municipal services, the population of the city. More than 200 individual houses were destroyed, in which more than 1000 families lived, factories were stopped, there were human casualties. According to the catalog compiled by us at the Institute of Hydrometeorology of Georgia, material damage from strong winds on November 16-17, 1961 amounted to USD 2 million, and on March 4, 1973, damage from a hurricane wind in the Tbilisi-Bolnisi region amounted to USD 5 million. The intense heat and drought caused damage to the city of Tbilisi and its regions in April-May 1997, 20 million, in May 2000 – 150 million, and in June 2001 – 10 million US dollars, etc. To mitigate the expected negative consequences of hazardous phenomena and unfavorable weather conditions, the associated potential risks should be assessed and compared with the value of the permissible risk and then decisions on adaptation should be made (Kobysheva et al., 2015). This article presents the results of a study of the most typical hazardous weather phenomena and assesses the climatic risks they create in the city of Tbilisi, the most important industrial, social and cultural center of the Caucasus.

2. Materials and methods

Climate risk is a combination of the likelihood and consequences of a hazardous or adverse event occurring. Risk is defined as the product of the probability of a particular meteorological hazard by the conditional probability of the vulnerability of the recipient who may be exposed to this hazard (Kobysheva et al., 2015):

$$R = pU \quad (1)$$

where: p is the probability of an event; U – the consequences of an event or the vulnerability of an object exposed to a hazardous phenomenon, which is determined by the formula:

$$U = (s / S) \cdot m \cdot t \cdot K \quad (2)$$

s is the average area of influence of this phenomenon (sq. km),

S - the area of the administrative region (sq. Km),

m is the population of the administrative region (people),

t is the time of action of a dangerous meteorological phenomenon or unfavorable weather conditions (days);

K is the coefficient of aggressiveness of the phenomenon.

Vulnerability depends on the geography and the degree of development of the affected area. The more developed the economy, the more damage occurs when dangerous phenomena pass through it. Climate risk is usually called social risk, i.e. the risk of social damage to the territory under consideration, since it determines the size of the population affected by this phenomenon.

The general formula of social risk or the likelihood of injury to a particular recipient is as follows (Kobysheva et al., 2008; Kobysheva et al., 2015):

$$Rc = p (s / S) \cdot m \cdot t \cdot K \quad (3)$$

The basis of the economic risk management mechanism is the definition of economic damage caused by a hazardous event. The cumulative damage in a given area is called economic risk. Economic risk is the product of the probability of a meteorological hazard by the amount of damage; expressed in monetary units (Kobysheva et al., 2008; Kobysheva et al., 2015):

$$Re = ARc \quad (4)$$

where A is the share of gross domestic product per day per inhabitant of a given administrative region. The article discusses the weather phenomena that create emergency situations in the city:

- Hot days (SU25 when the maximum air temperature exceeds 25° C).
- Strong wind (W, when the wind speed is not less than 15m / s).
- Heavy precipitation (R30, when the daily precipitation is at least 30 mm).
- Fog (F).
- Hail (Ha).
- Blizzard (B).

The materials of observations of the Tbilisi Hydrometeorological Observatory for the period 1961–2020 were used. All calculations were performed in accordance with the methods developed under the guidance of Kobysheva (Kobysheva et al., 2008; Kobysheva et al., 2015). The aggressiveness coefficients of the phenomena are determined in accordance with (Kobysheva et al., 2015), and the areas of influence of this phenomenon are taken from our previous studies (Elizbarashvili et al., 2013; Elizbarashvili et al., 2012; Elizbarashvili, Elizbarashvili, 2012; Elizbarashvili et al., 2020; Varazanashvili et al., 2012). Since meteorological phenomena are seasonal in nature, the calculations were performed separately for each season. In a number of cases, in the conditions of Georgia, the recipient is often affected by a complex of hazardous processes or their combination, which creates a complex risk. According to the main provisions of the theory of probability, the probability of a complex of independent events x and y can be calculated using the probability multiplication theorem (Elizbarashvili et al., 2020):

$$p(xy)=p(x)p(y), \tag{5}$$

where p (x) is the probability of an event x, p (y) is the probability of an event y.

3. Discussion

Table 1 shows the daily probabilities of some dangerous weather phenomena in Tbilisi and the corresponding aggressiveness coefficients.

Table 1. Daily probabilities of some dangerous weather phenomena and the aggressiveness coefficients of the phenomenon

| Weather phenomenon | Season | | | | K |
|--------------------|--------|--------|--------|--------|------|
| | Winter | Spring | Summer | Autumn | |
| SU25 | 0 | 0.24 | 0.83 | 0.38 | 0.02 |
| W | 0.06 | 0.08 | 0.04 | 0.04 | 1 |
| R30 | 0 | 0.02 | 0.02 | 0.01 | 0.03 |
| F | 0.22 | 0.02 | 0 | 0.13 | 0.5 |
| Ha | 0 | 0.01 | 0.01 | 0 | 3 |
| B | 0.002 | 0 | 0 | 0 | 0.08 |

It follows from Table 1 that hot days are the most common of the considered phenomena. Even in spring and autumn, their probability is quite high, and in summer it reaches 0.83. There is a high probability of fog during the cold season. Strong winds are recorded in all seasons. Their probability is not very high, however, it is characterized by a significant coefficient of aggressiveness. Hail is especially aggressive; it occurs during the warm season. The likelihood of a blizzard is insignificant.

Table 2 presents data on social and economic risks from hazardous weather phenomena, calculated according to formulas (3) and (4). When calculating the economic risk, the gross domestic product (GDP) was taken as USD 30 (in 2019 prices).

Table 2. Social (Rs people) and economic (Re US dollars in 2019 prices) risks from one phenomenon

| Weather phenomenon | Season | | | | | | | |
|--------------------|--------|---------|--------|---------|--------|---------|--------|---------|
| | Winter | | Spring | | Summer | | Autumn | |
| | Rc | Re | Rc | Re | Rc | Re | Rc | Re |
| SU25 | 0 | 0 | 5347 | 160410 | 18492 | 554760 | 8466 | 253980 |
| W | 66840 | 2005200 | 89120 | 2673600 | 44560 | 1336800 | 44560 | 1336800 |
| R30 | 0 | 0 | 668 | 20040 | 668 | 20040 | 334 | 10020 |
| F | 122540 | 3676200 | 11140 | 334200 | 0 | 0 | 77980 | 2339400 |
| Ha | 0 | 0 | 322 | 9660 | 322 | 9660 | 0 | 0 |
| B | 1.2 | 36 | 0 | 0 | 0 | 0 | 0 | 0 |

Social risk indicates the number of people affected at a certain level, it characterizes the severity of the consequences (catastrophic) of the implementation of hazards. Table 2 shows that the distribution of social risks is seasonal. Fog and strong winds pose the greatest risks to the city as a whole. In particular, the greatest risk from fog is expected mainly in the autumn-winter period, in spring it decreases, and in summer it is absent. The social risk from strong winds is greatest in spring, although the risk is also significant for other seasons. The economic risk is also greatest from fog and strong winds. For example, in winter, the economic risk from fog in one case can be more than \$ 3.6 million, in autumn – more than \$ 2.3 million. The economic risk from strong winds in spring exceeds \$ 2.6 million and in winter exceeds \$ 2 million. Figure 1 shows the daily probabilities of the joint realization of some dangerous meteorological phenomena in the city by the seasons of the year, calculated by the formula (5).

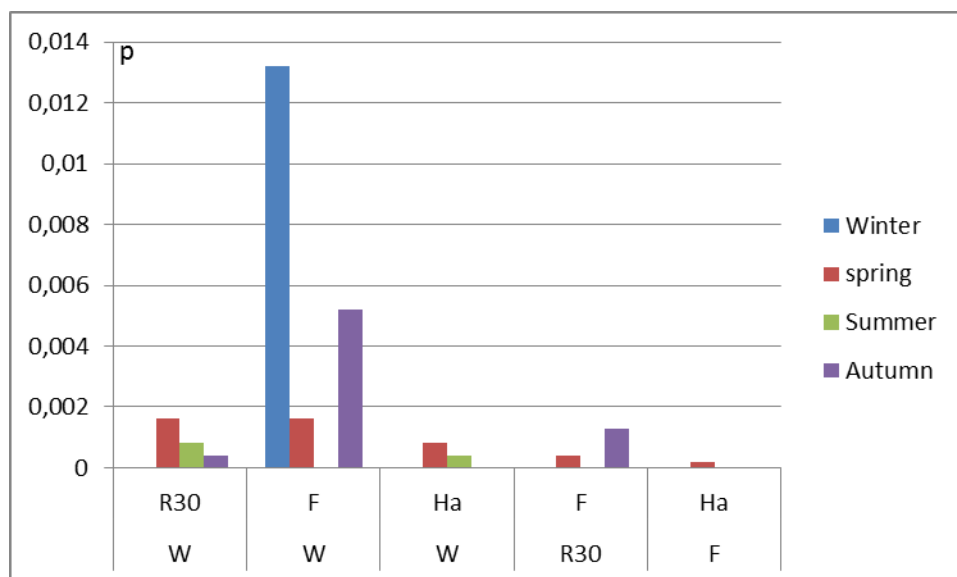


Fig. 1. Probability of joint realization of some dangerous weather phenomena

It follows from Figure 1 that the probability of joint realization of some dangerous weather phenomena is very low, however, a fog-strong wind (F-W) complex stands out, the probability of which significantly exceeds the probability of other complexes, especially in the autumn-winter season.

Accordingly, social and economic risks are significant in the implementation of this complex of phenomena, reaching more than 22 thousand people and about 700 thousand US dollars in winter, respectively (Table 3).

Table 3. Social (Rs people) and economic (Re US dollars in prices of 2019) risks from a complex of phenomena

| Complex of weather phenomena | Season | | | | | | | |
|------------------------------|--------|--------|--------|--------|--------|-------|--------|-------|
| | Winter | | Spring | | Summer | | Autumn | |
| | Rc | Re | Rc | Re | Rc | Re | Rc | Re |
| R30 - W | 0 | 0 | 1840 | 55200 | 920 | 27600 | 460 | 13800 |
| F - W | 22770 | 683100 | 2760 | 82800 | 0 | 0 | 920 | 27600 |
| Ha - W | 0 | 0 | 3680 | 110400 | 1840 | 55200 | 0 | 0 |
| F - R30 | 0 | 0 | 230 | 6900 | 0 | 0 | 805 | 24150 |
| Ha - F | 0 | 0 | 805 | 24150 | 0 | 0 | 0 | 0 |

From Table 3 it follows that certain risks are also created during the implementation of other complexes.

4. Conclusion

1. The most common of the phenomena considered are hot days. Even in spring and autumn their probability is quite high, and in summer it reaches 0.83. There is a high probability of fog during the cold season. Strong winds occur in all seasons. Their probability is not very high, but is characterized by a significant coefficient of aggressiveness. Hail is especially aggressive and occurs during the warm season. The likelihood of a snowstorm developing is insignificant.

2. The distribution of social risks is seasonal. The greatest risk for the city as a whole is fog and strong winds. In particular, the greatest risk from fog is expected mainly in the autumn-winter period; it decreases in the spring and is absent in the summer. The social risk from strong winds is greatest in the spring, although in other seasons the risk is also significant.

3. Economic risk is also greatest from fog and strong winds. For example, in winter the economic risk from fog per incident can be more than 3.6 million US dollars, in the fall - more than 2.3 million US dollars. The economic risk from strong winds in spring exceeds \$2.6 million, and in winter exceeds \$2 million.

References

Elizbarashvili, Elizbarashvili, 2012 – Elizbarashvili, E.Sh., Elizbarashvili, M.E. (2012). Stikhiinye meteorologicheskie yavleniya na territorii Gruzii [Natural meteorological phenomena on the territory of Georgia]. Tbilisi. 104 p. [in Russian]

Elizbarashvili et al., 2020 – Elizbarashvili, E.Sh., Elizbarashvili, M.E., Elizbarashvili, Sh.E. (2020). Investigation of the frequency of occurrence of the most dangerous meteorological phenomena for Georgia. *Russian Meteorology and Hydrology*. 45(10): 727-732. DOI: 10.3103/S1068373920100076

Elizbarashvili et al., 2019 – Elizbarashvili, E.Sh., Elizbarashvili, M.E., Elizbarashvili, Sh.E., Pipia, M.G., Chelidze, N.Z. (2019). Catastrophic Precipitation in Georgia. *European Geographical Studies*. 6(1): 50-60. DOI: 10.13187/egs.2019.1.50

Elizbarashvili et al., 2020 – Elizbarashvili, E.Sh., Elizbarashvili, M.E., Elizbarashvili, Sh.E., Pipia, M.G., Kartvelishvili, L.G. (2020). Blizzards in Mountain Regions of Georgia. *Russian Meteorology and Hydrology*. 45: 58-62. DOI: 10.3103/S1068373920010082

Elizbarashvili et al., 2013 – Elizbarashvili, E.Sh., Varazanashvili, O.Sh., Tsereteli, N.S., Elizbarashvili, M.E. (2013). Hurricane winds in the territory of Georgia. *Russian Meteorology and Hydrology*. 38(3): 168-170. DOI: <https://doi.org/10.3103/S1068373913030047>

Elizbarashvili et al., 2012 – Elizbarashvili, E.Sh., Varazanashvili, O.Sh., Tsereteli, N.S., Elizbarashvili, M.E., Elizbarashvili, Sh.E. (2012). Dangerous fogs on the territory of Georgia. *Russian Meteorology and Hydrology*. 37(2): 52-59. DOI: <https://doi.org/10.3103/S1068373912020057>

Kobysheva et al., 2015 – Kobysheva, N.V., Akentieva, E.M., Galyuk, L.P. (2015). Climate risks and adaptation to climate change and variability in the technical sphere. St. Petersburg. 144p. [in Russian]

Kobysheva et al., 2008 – Kobysheva, N.V., Galyuk, L.P., Panfutova, Yu.A. (2008). Methodology for calculating social and economic risks created by dangerous weather phenomena. *Proceedings of the MGO*. 558: 162-172. [in Russian]

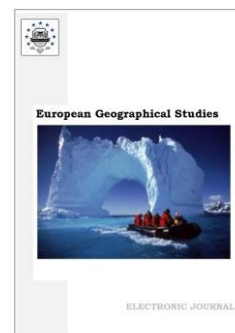
Varazanashvili et al., 2012 – Varazanashvili, O., Tsereteli, N., Amiranashvili, A., Tsereteli, E., Elizbarashvili, E., Dolidze, J., Qaldani, L., Saluqvadze, M., Adamia, S., Arevadze, N., Gventcadze, A. (2012). Vulnerability, hazards and multiple risk assessment for Georgia. *Natural Hazards*. 64: 2021-2056. DOI 10.1007/s11069-012-0374-3

Copyright © 2023 by Cherkas Global University



Published in the USA
 European Geographical Studies
 Issued since 2013.
 E-ISSN: 2413-7197
 2023. 10(1): 8-18

DOI: 10.13187/egs.2023.1.8
<https://egs.cherkasgu.press>



Statistical Characteristics of Hurricane Winds over Georgia for the Period 1961–2022

Elizbar Sh. Elizbarashvili ^{a, *}, Otar Sh. Varazanashvili ^b, Avtandil G. Amiranashvili ^b,
 S. Fuchs ^c, Tsisana Z. Basilashvili ^a

^a Georgian Technical University, Institute of Hydrometeorology, Georgia

^b Ivane Javakhishvili Tbilisi State University, Mikheil Nodia Institute of Geophysics, Georgia

^c University of Natural Resources and Life Sciences, Institute of Mountain Risk Engineering, Vienna, Austria

Abstract

A catalog of hurricanes over the territory of Georgia for the period 1961–2022 has been compiled, containing the period of onset, geographical coordinates of the epicenter, speed, magnitude, intensity, area of distribution, material damage, human casualties. Over the entire study period, about 1600 cases of hurricane winds were recorded. During the year, hurricanes occur on average 20 times, with the highest number of cases recorded in 2002 – 81. The average speed of hurricane winds in general for Georgia is 36 m/s, the highest speed reached 56 m/s. The average hurricane area is about 1200 sq. km, and the maximum hurricane area exceeds 10000 sq. km. There is no clear relationship between the hurricane area and the corresponding material damage, which can most likely be explained by the heterogeneity of the level of urbanization of comparable areas that experience varying degrees of damage. The long-term changes in hurricane activity reveal a cyclical nature, which can be explained by the peculiarities of atmospheric circulation. In general, over the entire period there has been a tendency for hurricane activity to weaken.

Keywords: hurricane, speed, intensity, magnitude, frequency.

1. Introduction

Hurricanes are deadly and serious events, making it important to understand their regional characteristics and assess the long-term risk they pose to society. In connection with this study, a large literature is devoted to these phenomena, which examines various problems of climatology, research and forecasting of hurricane winds in various parts of the Globe. In particular, hurricane wind speeds are assessed for the Southeastern United States region, including South Carolina, North Carolina and eastern Virginia (Lee, Rosovsky, 2007), the risk of dealing with high and hurricane winds in Florida cities (Malmstadt et al., 2010), analyzed changes in the average and maximum wind speed, the number of days with strong winds over China (Jiang et al., 2010), examined the features of the conditions of squalls and tornadoes observed in the European part of Russia (Chernokulsky et al., 2022), analyzed long-term fluctuations in wind speed in Czech Republic (Brazdil et al., 2009), climatology and wind speed trends in Australia were studied (McVicar et al., 2008), hurricane wind speeds along the Persian Gulf and the east coast of the USA

* Corresponding author

E-mail addresses: eelizbar@hotmail.com (E.Sh. Elizbarashvili),
otarivar@yahoo.com (O.Sh. Varazanashvili), avtandilamiranashvili@gmail.com (A.G. Amiranashvili),
gaprindashvili.george@mail.com (G.M. Gaprindashvili), jarjnio@mail.ru (Ts.Z. Basilashvili)

were simulated using Monte Carlo method (Xu et al 1980; Batts Martin et al., 1980), solved hurricane equations of motion for use in high-speed simulations (Vickery et al., 2000), and reviewed climatological models of extreme hurricane winds for the entire US coastline, as well as the Gulf, Florida, and East Coasts (Jagger, Elsner, 2006), a forecast of hurricane winds of extratropical cyclones in Russia was carried out (Aleksseva, 2017), using all hurricanes of 2003 and 2004 in the Atlantic and Gulf of Mexico, a hurricane wind forecast model was developed (Xie et al., 2006), etc. Hurricane winds cause significant damage to the economy and population of Georgia: they damage communication and power lines, disrupt transport, cause disturbances in the sea and reservoirs, dust storms, snow transport, avalanches, soil erosion and other adverse phenomena, and sometimes cause loss of life. On the territory of Georgia, hurricane winds are mainly in the western or eastern direction. The first of them occur when a cyclone of Mediterranean origin or a deep trough of low pressure associated with Atlantic cyclones passes over Transcaucasia. At the same time, the pressure gradient is directed from west to east, which causes an increase in western and northwestern winds. Eastern winds are observed when a high pressure area is established over the central and eastern regions of Transcaucasia, and a cyclone spreads to the Black Sea from the west. In this case, the pressure gradient is directed from east to west, and eastern winds, which are most developed in Western Georgia, intensify (Elizbarashvili, Elizbarashvili. 2012). Research on strong, including hurricane, winds in the territory of Georgia also has a long history, although the most relevant work has been carried out in recent years. In the article (Elizbarashvili et al., 2013) for the period 1961–2008, the statistical structure of hurricane winds was studied, the number of days and duration of hurricane winds were determined, the empirical functions of their distribution and the size of their habitats were studied, and the geography, the structure, areas and dynamics of natural meteorological phenomena, including hurricane winds, and in the article (Varazanashvili et al., 2012) the spatial distribution of hurricane winds was assessed, the maximum economic losses were calculated, and a map of expected risks was constructed. This article, which was financially supported by the Shota Rustaveli National Science Foundation (grant No. FR-21-1808, 2022–2024), is a logical continuation of these studies. It presents the results of a study of the statistical characteristics of hurricane winds over Georgia for the period 1961–2022.

2. Materials and methods

The research methodology included: 1. Compilation of a catalog of hurricane winds for the period 1961–2022; 2. Study of the spatial and temporal characteristics of hurricane winds. In preparing the catalog, all available information was used (observation materials from the National Environmental Agency of Georgia for the period 1961–2022, personal archives, literary records and manuscripts, printed and electronic media and other materials). These data comply with World Meteorological Organization standards. All measurements were carried out at a height of 10 m above the ground surface. Regular meteorological observations in Georgia began in 1844. By the beginning of the 20th century, about 30 weather stations were operating, and in the 40s their number reached about 160. By the beginning of the 90s, observations were carried out at more than 120 meteorological stations, and by the end of the 90s, due to the collapse of the USSR, the number weather stations decreased to 50. In 2005–2010, about 20 weather stations operated in Georgia, and currently their number is less than 50 (Elizbarashvili et al., 2013a).

The principles of compiling catalogs of hazardous natural phenomena, including hurricane winds, and the classification of magnitudes are discussed in detail in our previous article (Varazanashvili et al., 2022).

The preparation of materials for the catalog was carried out in several stages: at the first stage, factual data was collected and systematized, then primary data processing was carried out, calculation of various hurricane parameters and compilation of a chronological basis in which all the prepared data, as well as the results of their primary analysis, were entered in strict order. processing. In total, observational materials from 50 weather stations were used for the period 1961–2022. As a result, a catalog of hurricanes was compiled containing such indicators of the phenomenon as the period of occurrence (year, month, day), geographical coordinates of the epicenter (latitude, longitude), speed (V_m/s), magnitude (M), intensity (I) and area hurricane spread (Sq.km), material damage (Q US dollars X1000), human casualties (Varazanashvili et al. 2023).

The magnitude of a hurricane was determined as a value proportional to wind speed, the proportionality coefficient was conventionally taken as 0.1. Magnitude expresses the strength of

a hurricane. The intensity of the hurricane was determined according to the scale we developed earlier (Varazanashvili et al., 2012) (Table 1).

Table 1. Hurricane intensity scale (Varazanashvili et al., 2012)

| Intensity balls | wind speed m/s | Effect | Economic losses in US dollars per unit area (km ²) |
|-----------------|----------------|-------------|--|
| 1 | 30–34 | Weak | 100 |
| 2 | 35–40 | Average | 101–1000 |
| 3 | 40–45 | Strong | 1 001–5 000 |
| 4 | >45 | Very strong | >5000 |

From Table 1 it can be seen that, depending on the wind speed, there are 4 types of hurricane wind intensities: weak, medium, strong and very strong. Hurricane activity was assessed by its frequency (N) over a certain period of time (number of cases).

Such catalogues-databases were compiled by different authors, for example in (Lee, Rosowsky, 2007). For the southeastern United States, a database has been compiled that includes time index (year), duration of strong winds and peak surface wind speeds (both gusty and sustained), etc.

The study of the temporal and spatial patterns of the characteristics of hurricane winds implied the determination of the frequency and range of hurricanes, and the identification of patterns of their spatio-temporal distribution.

Long-term changes in the frequency and magnitude of hurricane winds were assessed using the moving average method. This made it possible to smooth out short-term fluctuations and highlight the main trends in their change (Bulashev, 2003). The moving average is numerically equal to the arithmetic mean of the values of the original function over a specified period. The resulting moving average value in climatology is referred to as the middle of the selected interval.

3. Discussion

In accordance with the developed catalog, about 1,600 cases of hurricane winds were recorded in Guzia. Thus, during the year, hurricanes occur on average 20 times; their largest number of cases was recorded in 2002 – 81. The most probable (46 %) are up to 20 cases of hurricanes per year, gradations of 21-40 and 41-60 cases correspond to a frequency of 26 and 23 %, and gradations of 61-80 and more than 80 are observed in 3 and 2 % of cases, respectively (Figure 1).

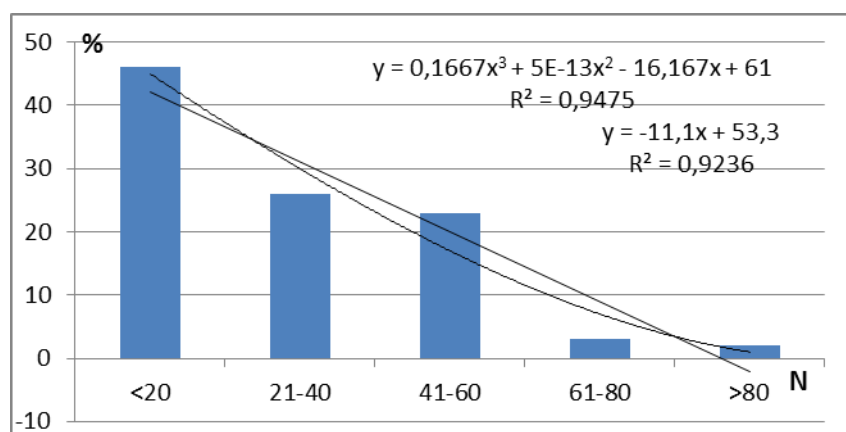


Fig. 1. Repeatability of the number of cases of hurricane winds on the territory of Georgia per year and its approximation by a 3rd degree polynomial and linear function (R² – determination coefficient)

From Figure 1 it follows that the coefficient of determination in both cases is very high (>0.9), however, the empirical distribution of the number of hurricane winds is better

approximated by a third-degree polynomial than by a linear function. In the first case, the coefficient of determination is 0.94, and in the second case it is 0.92.

Table 2 provides information on the most catastrophic hurricanes. As follows from the table, the capital of Georgia is one of the most hurricane-prone cities. For example, in 2005–2006 alone, 4 hurricanes with wind speeds of more than 50 m/s were recorded in Tbilisi.

Table 2. Most intense hurricanes

| Speed, m/s | Epicenter | Year | Month | Date | Square distribution sq.km |
|------------|----------------|------|-------|------|---------------------------|
| 56 | Zekari, Udabno | 1981 | 2 | 3 | 9000 |
| 55 | Tbilisi | 2005 | 4 | 20 | 1200 |
| 53 | Tbilisi | 2006 | 3 | 10 | 1400 |
| 52 | Tbilisi | 2006 | 9 | 16 | 1200 |
| 51 | Tbilisi | 2005 | 3 | 4 | 1200 |

The average speed of hurricane winds in general for Georgia is 36 m/s, the highest speed is 56 m/s, the average hurricane intensity is 1.57, and the maximum intensity is 4 points. The average hurricane area is about 1200 sq. km, and the maximum hurricane area exceeds 10000 sq. km. In general, hurricanes with intensity 1 and 2 points predominate in the territory of Georgia, the frequency of each of them is 48 %. These are hurricanes of weak and medium intensity with a speed of 40 m/s or less. Their total repeatability is 96 %. The remaining 4 % of hurricane cases are hurricanes of strong (40–45 m/s) and very strong (more than 45 m/s) intensity, accounting for 3 and 1 %, respectively (Figure 2).

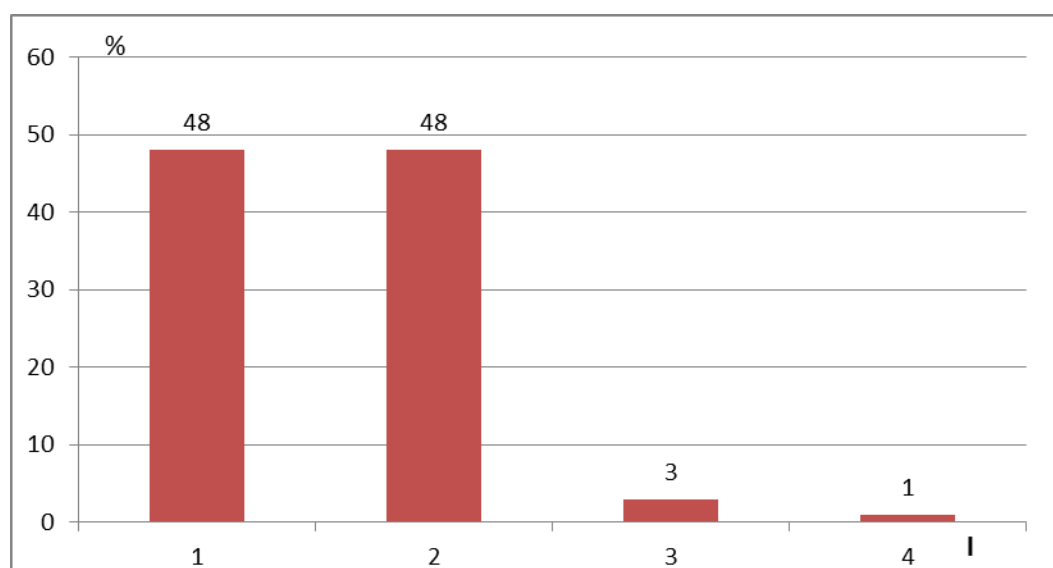


Fig. 2. Frequency of hurricane winds of varying intensity

The hurricane area varies widely (Figure 3). The average area of distribution of a hurricane of low intensity (point 1) is more than 1,500 sq. km, although the range of fluctuations is significant (100–10000 km). The area of distribution of a hurricane with average intensity (2 points) is on average about 2400 sq. km., with a similar amplitude of fluctuations. The average area of a hurricane with strong intensity (3 points) is more than 1000 sq. km (varies between 400–6000 sq. km), and the average area of a hurricane with very strong intensity (4 points) is about 1600 sq. km. (400–9000 sq.km.).

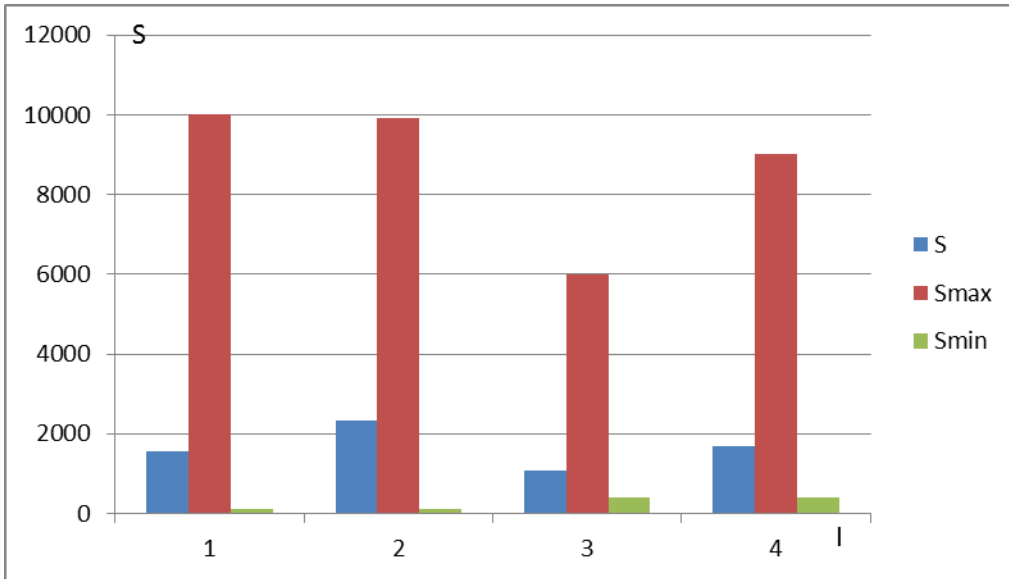


Fig. 3. Hurricane area of varying intensity (sq. km); S-average; Smax-largest; Smin-smallest

Figure 4 shows an empirical histogram of the frequency of occurrence of hurricane winds of varying intensity. From Fig. It follows that hurricane-force winds can cover an area of several thousand square kilometers, but hurricanes are most likely to occur with an area of less than 2000 square kilometers. Frequency of habitats with an area of less than 1000 square kilometers, depending on their intensity, ranges from 42-49 %, and the frequency of habitats with an area of 1000-2000 sq. km ranges from 27-44 %. The frequency of occurrence of areas of other gradations is significantly less.

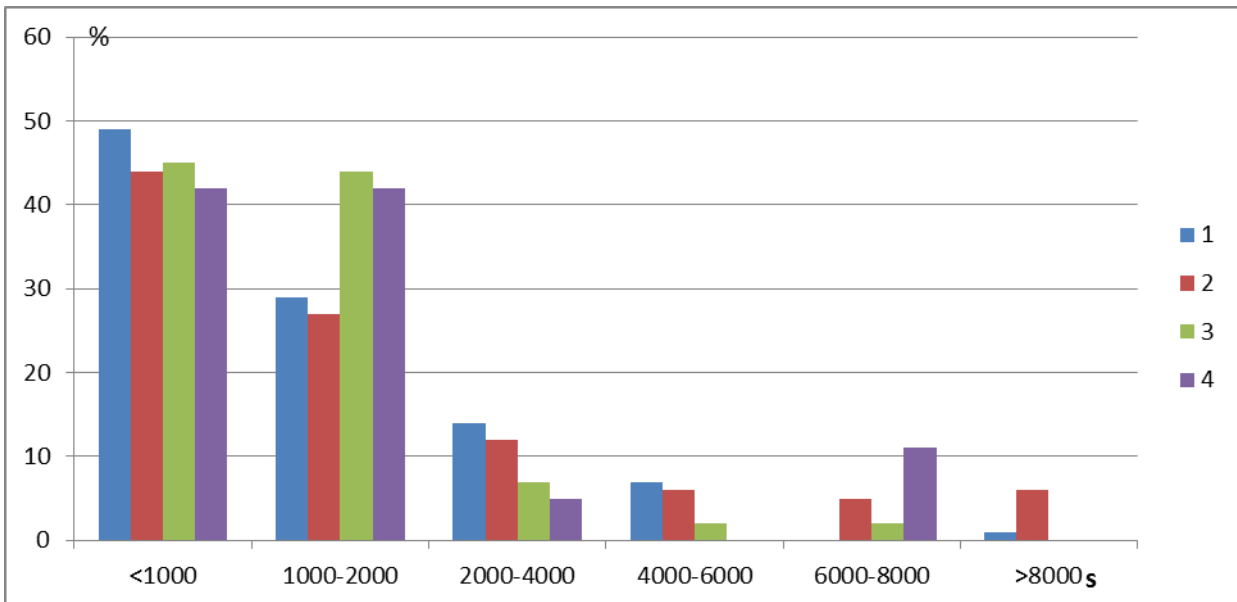


Fig. 4. Histogram of the frequency of occurrence of hurricane winds of varying intensity: I = 1; I = 2; I = 3; I = 4.

In addition, from Figure 4 it follows that on an area of less than 1000 sq. km are dominated by hurricanes of low intensity (about 50 %), with wind speeds of less than 34 m/s. On an area of 1000-2000 sq. km, hurricanes of strong and very strong intensity most often spread, the frequency of each of them is more than 40 %. The speed of such hurricanes exceeds 40 m/s. On a large area, more than 6000 sq. km, hurricanes of very strong and medium intensity are predominant.

In general, the frequency of occurrence of hurricanes of varying intensity naturally decreases with increasing area of the area, with the exception of hurricanes of very strong intensity, the frequency of which over large areas (6-8 thousand sq. km.) slightly increases. According to our estimates, hurricanes spreading over an area of 8-10 thousand square meters. km or more can cause material damage up to 10 million US dollars.

At the same time, there is no clear relationship between the hurricane area and the corresponding material damage, which can most likely be explained by the heterogeneity of the level of urbanization of comparable areas that experience damage of varying degrees (Figure 5).

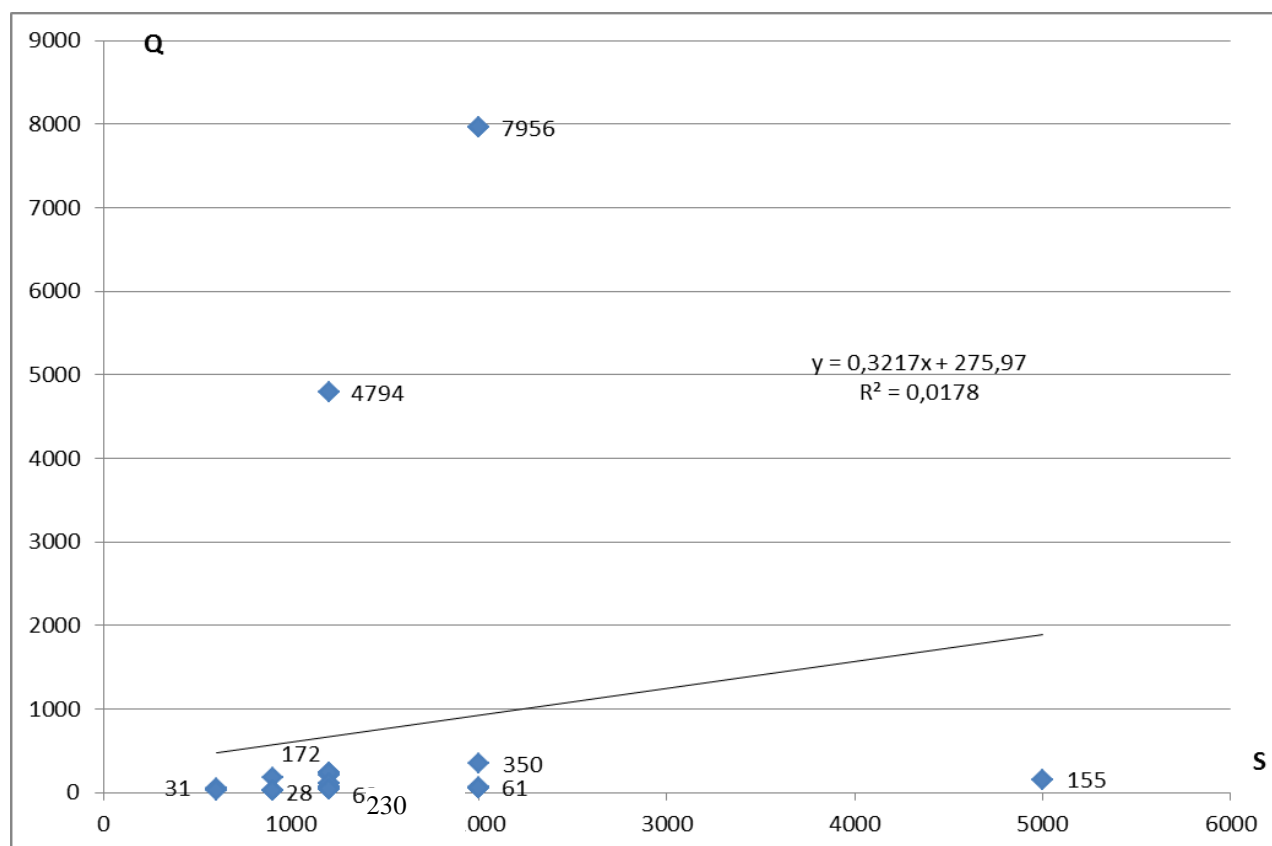


Fig. 5. The relationship between the area of hurricane spread (S sq. km) and the corresponding material damage (Q thousand dollars), and its approximation by a linear function (R^2 – coefficient of determination) for the period 1995–2002

The relationship presented in Figure 5 is very weak $R^2 = 0.017$, this means that the material damage caused by a hurricane is only 1-2 % due to differences in the hurricane's areas of action, and 98-99 % is due to the influence of other factors. The first factor among these factors is the level of urbanization.

The geographic distribution of the characteristics of hurricane winds is complex and depends not only on general physical and geographical conditions, but also to a large extent on local conditions (Table 3).

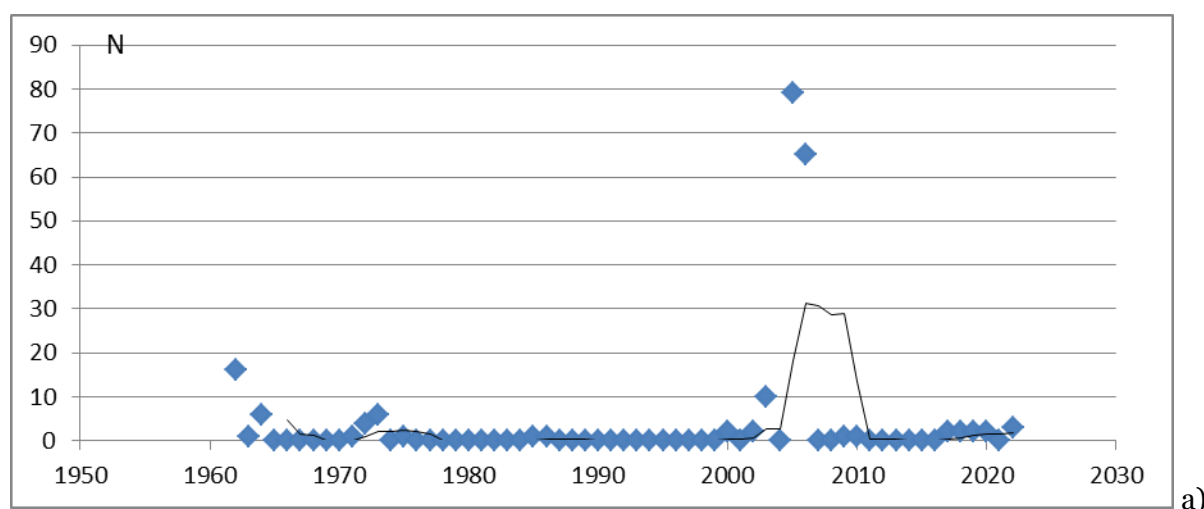
In Table 3, N is the average frequency of hurricanes per year (number of events), Nmax is the highest frequency of hurricanes per year (number of events), Mmax is the highest magnitude, a dash in the table means that this value was observed several times. . From Table 3 it follows that the highest frequency of hurricane winds is typical for the Kvemo Kartli region (Udabno, Tbilisi), where it amounts to 4.4 and 3.7 cases on average per year, respectively. In the Colchis Lowland, the frequency of hurricane winds is somewhat less (Kutaisi, Senaki, 2.5-1.8 cases). The frequency of hurricane winds is significantly lower in the South Georgian Plateau, where it does not reach 1 case on average per year. Large frequency values are typical for the passes (Mamisonsky, Goderdzsky, Zekarsky, 1.4-2.5 cases). The highest magnitudes of hurricane magnitudes are also characteristic of

Kvemo Kartli, the Colchis lowland and mountain pass areas (on average 1-2 points or more), and the lowest magnitudes are characteristic of the South Georgian Highlands (less than 1).

Table 3. Some characteristics of hurricane winds in various physical and geographical conditions

| Region | Paragraph | | | | | |
|-------------------------------------|--|------|------|------|------|-----------|
| | | N | Nmax | Year | Mmax | Year |
| Black Sea coast and Colchis Lowland | Kutaisi Senaki Batumi | 2,5 | 14 | 1977 | 4,6 | 1970 |
| | | 1,8 | 9 | 1993 | | 1993 |
| | | 0,2 | 2 | 1976 | 4,5 | - |
| Kvemo Kartli | Udabno Tbilisi Bolnisi | 0,2 | 2 | | 4 | |
| | | 4,4 | 34 | 1990 | 4,1 | 1973 |
| | | 3,7 | 79 | 2005 | 5,5 | 200 |
| | | 0,1 | 2 | 2013 | 3,5 | 5 2013 |
| South Georgian Highlands | Akhaltsikhe Akhalkalaki Paravani | 0,08 | 4 | 1972 | 4 | 1972 |
| | | 0,06 | 1 | - | 4 | 1972 |
| | | 0,13 | 3 | 1977 | 3,4 | - |
| Passes | Mamisoni Goderdzi Zekari | 2,4 | 17 | 1973 | 4,3 | 1969 |
| | | 1,4 | 8 | 1961 | 4 | - |
| | | 1,5 | 9 | 1990 | 4,1 | 1973 |

In Figures 6 and 7 presents the long-term course of changes in the frequency and maximum magnitude of hurricanes for 3 weather stations characterized by high hurricane danger, covering various physical-geographical and climatic conditions: Tbilisi-plain part of Eastern Georgia (404 m above sea level), Kutaisi-Colchis lowland (114m above sea level) .a.s.l.), Mta Sabueti-Likhsy ridge (1242m a.s.l.).



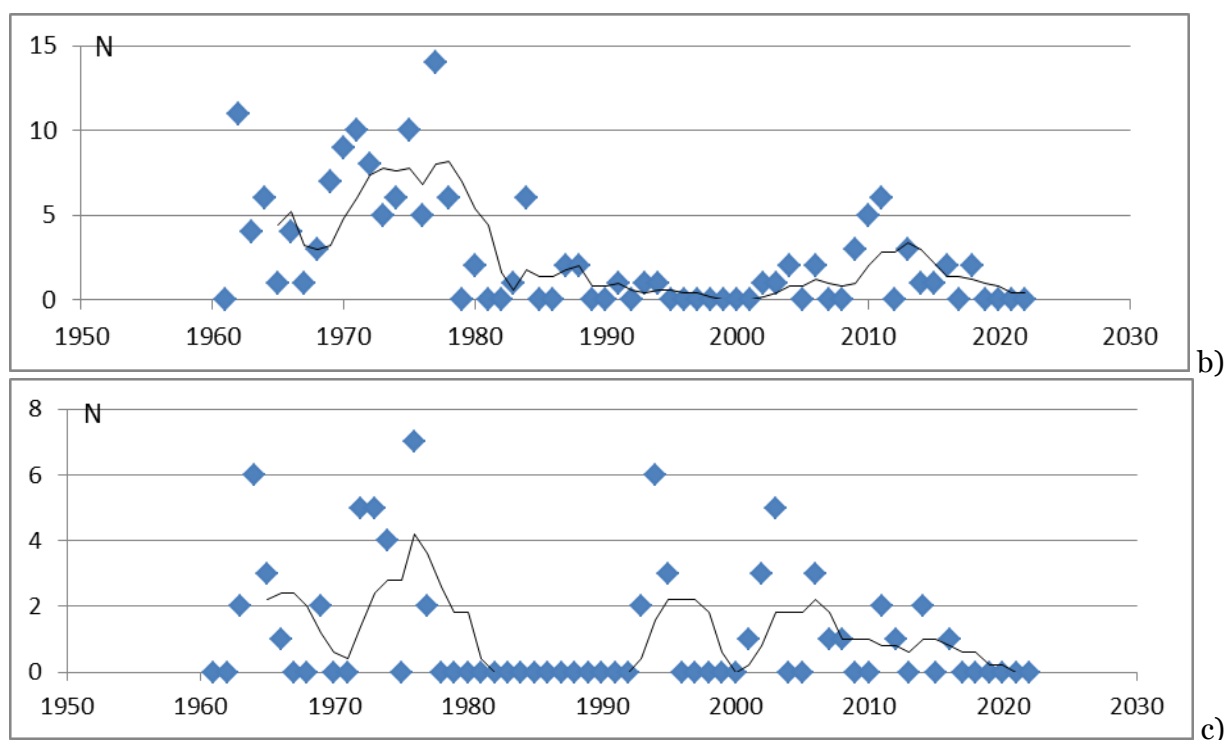
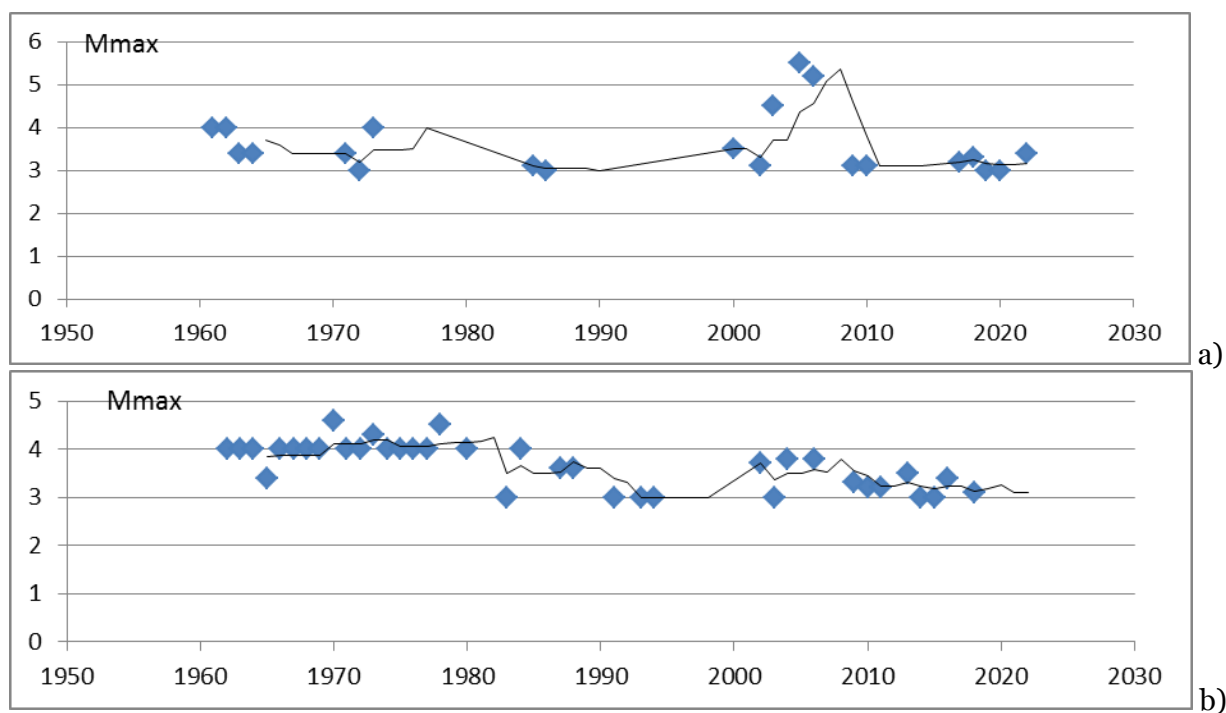
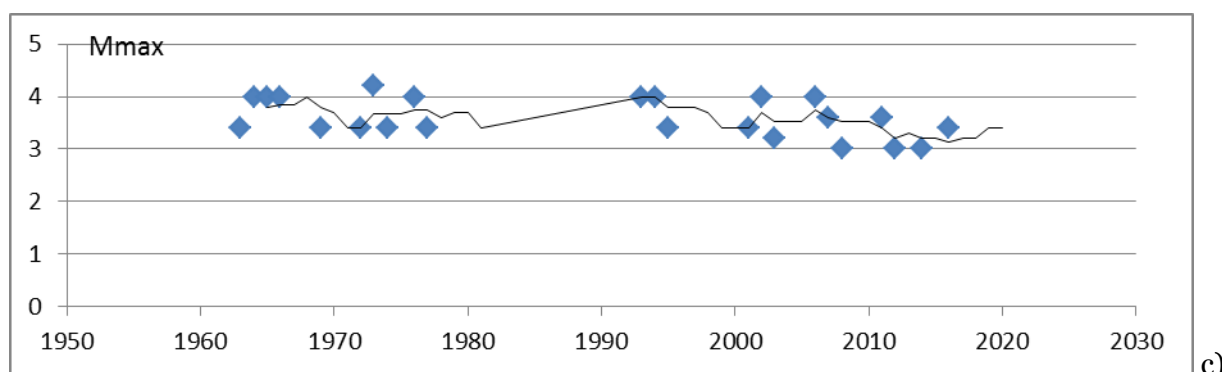


Fig. 6. Long-term changes in frequency (N) of hurricanes: annual data and 5-year moving averages: a) Tbilisi; b) Kutaisi; c) Mta Sabueti





c)

Fig. 7. Long-term changes in maximum magnitude (Mmax) of hurricanes: annual data and 5-year moving averages: a)- Tbilisi; b)- Kutaisi; c)- Mta Sabueti

From [Figures 6 and 7](#) it follows that the annual data on the frequency and maximum magnitude of hurricanes are widely scattered, while moving averages, which are obtained by smoothing short-term fluctuations, make it possible to identify the main trends in their changes. According to [Fig. 6](#), changes in hurricane activity reveal a cyclical nature. The first maximum in the long-term course of hurricanes was observed in the 60s of the last century, the second in 1970–1975, the third in 2000–2010. In Mta-Sabueti, the maximum is also detected at the end of the 90s. The same maximums generally correspond to the maximum magnitudes of hurricanes. In particular, in Tbilisi, the largest number of hurricane cases was noted for the period 2000–2010, the highest magnitude of 5.6 corresponds to the same period. During the same cycle in Kutaisi and Mga Sabueti, the frequency of hurricanes is 5-6 cases per year, and the highest magnitude reaches 4 points. In Kutaisi and Mga Sabueti, the main maximum in the frequency and magnitude of hurricanes is observed in 1970–1975 and amounts to up to 14 cases in Kutaisi, with a maximum magnitude of 4.6, and in Mta Sabueti 6-7 cases per year, with a magnitude of 4.2 points. The cyclical nature of changes in hurricane activity can be explained by the peculiarities of atmospheric circulation. The decrease in the activity of hurricane winds after the 60s may be caused by the weakening of the zonal and strengthening of the meridional circulation of the atmosphere, and the increased activity of hurricanes in the 70s and 90s may be caused by the increased activity of the eastern form of atmospheric circulation in those years. The increase in the frequency of hurricanes in 2000-2010 may be caused by the intensification of the western form of atmospheric circulation ([Long-term changes..., 2001](#)).

In general, over the entire period there is a certain tendency for hurricane activity to weaken, which cannot be said for the maximum magnitude. In addition, the long-term course of hurricane activity in the considered locations has an individual character, which is formed by local physical-geographical and climatic features.

4. Conclusion

1. A catalog of hurricanes has been compiled, containing the period of occurrence (year, month, date), geographical coordinates of the epicenter (latitude, longitude), speed (Vm/s), magnitude (M), intensity (I), area of distribution (S sq. km), property damage (Q US dollars X1000), loss of life.

2. During the period 1961-2022, about 1,600 cases of hurricane winds were recorded. During the year, hurricanes occur on average 20 times, with the highest number of cases recorded in 2002 – 81. The most probable (46 %) are up to 20 cases of hurricanes per year, gradations of 21-40 and 41-60 cases correspond to a frequency of 26 and 23 %, and gradations of 61-80 and more than 80 are observed in 3 and 2 % of cases, respectively

3. The average speed of hurricane winds in general for Georgia is 36 m/s, the highest speed reached 56 m/s, the average hurricane intensity is 1.57, and the maximum intensity is -4 points. The average hurricane area is about 1200 sq. km, and the maximum hurricane area exceeds 10000 sq. km.

4. In general, hurricanes with intensity 1 and 2 points predominate in the territory of Georgia, the frequency of each of them is 48 %. These are hurricanes of weak and medium intensity

with a speed of 40 m/s or less. Their total repeatability is 96 %. The remaining 4 % of hurricane cases are hurricanes of strong (40-45 m/s) and very strong (more than 45 m/s) intensity, accounting for 3 and 1 %, respectively.

5. Hurricane-force winds can cover an area of several thousand square kilometers, but hurricanes are most likely to occur within an area of less than 2000 square kilometers. Frequency of habitats with an area of less than 1000 square meters. km, depending on their intensity, ranges from 42-49 %, and the frequency of habitats with an area of 1000-2000 sq. km ranges from 27-44 %. The frequency of occurrence of areas of other gradations is significantly less.

6. There is no clear relationship between the area of hurricane spread and the corresponding material damage, which in all likelihood can be explained by the heterogeneity of the level of urbanization of comparable areas that experience damage of varying degrees.

7. The long-term changes in hurricane activity reveal a cyclical nature, which can be explained by the peculiarities of atmospheric circulation. The first maximum during hurricanes was observed in the 60s of the last century, the second in 1970–1975, although weakly expressed in Tbilisi, the third in 2000–2010. In Mta-Sabueti, the maximum is also detected at the end of the 90s. The same maximums correspond to the maximum magnitudes of hurricanes.

8. Over the entire period, there is a certain tendency for hurricane activity to weaken, which cannot be said for the maximum magnitude. In addition, the long-term course of hurricane activity in the considered locations has an individual character, which is formed by local physical-geographical and climatic features.

References

- [Alekseeva, 2017](#) – *Alekseeva, A.A.* (2017). Forecasting hurricane winds in extratropical cyclones in Russia. *Russian Meteorology and Hydrology*. 42:1-8. DOI: <https://doi.org/10.3103/S1068373917010010>
- [Batts et al., 1980](#) – *Batts, M.E., Simiu, E., Russell, L.R.* (1980). Hurricane Wind Speeds in the United States. *Journal of the Structural Division*. 106(10): 269-280. DOI: doi.org/10.1061/JSDEAG.0005541
- [Brazdil et al., 2009](#) – *Brazdil, R., Chroma, K., Dobrovolny, P., Tolasz, R.* (2009). Climate fluctuations in the Czech Republic during the period 1961–2005. *International Journal of Climatology*. 29: 223-242. DOI: [10.1002/joc.1718](https://doi.org/10.1002/joc.1718)
- [Bulashev, 2003](#) – *Bulashev, S.V.* (2003). Statistika dlya treiderov [Statistics for traders]. M.: Company Sputnik +, 245 p. [in Russian]
- [Chernokulsky et al., 2022](#) – *Chernokulsky, A.V., Shikhov, A.N., Yarinich, Yu.I. et al.* (2022). Squalls and Tornadoes over the European Territory of Russia on May 15, 2021: Diagnosis and Modeling. *Russian Meteorology and Hydrology*. 47: 867-881. DOI: [10.3103/s1068373922110073](https://doi.org/10.3103/s1068373922110073)
- [Elizbarashvili, Elizbarashvili, 2012](#) – *Elizbarashvili, E.Sh., Elizbarashvili, M.E.* (2012). Stikhiinye meteorologicheskie yavleniya na territorii Gruzii [Natural meteorological phenomena on the territory of Georgia]. Tbilisi. 104 p. [in Russian]
- [Elizbarashvili et al., 2013](#) – *Elizbarashvili, E., Tatishvili, M., Elizbarashvili, M., Mesxia, R., Elizbarashvili, S.* (2013). Change of climate of Georgia in the conditions of global warming. Tbilisi, 138 p. [in Georgian]
- [Elizbarashvili et al., 2013a](#) – *Elizbarashvili, E.Sh., Varazanashvili, O.Sh., Tsereteli, N.S., Elizbarashvili, M.E.* (2013). Hurricane winds on the territory of Georgia. *Russian Meteorology and Hydrology*. 38(3): 168-170. DOI: [10.3103/S1068373911060069](https://doi.org/10.3103/S1068373911060069)
- [Jagger, Elsner, 2006](#) – *Jagger, Th.H., Elsner, J.B.* (2006). Climatology Models for Extreme Hurricane Winds near the United States. *Journal of Climate*. 19(13): 3220-3236. DOI: doi.org/10.1175/JCLI3913.1
- [Jiang et al., 2010](#) – *Jiang, Y., Luo, Y., Zhao, Z., Tao, S.* (2010). Changes in wind speed over China during 1956–2004. *Theoretical and Applied Climatology*. 99: 421-430. DOI: [10.1007/s00704-009-0152-7](https://doi.org/10.1007/s00704-009-0152-7)
- [Lee, Rosowsky, 2007](#) – *Lee Kyung Ho, Rosowsky, David V.* (2007). Synthetic Hurricane Wind Speed Records: Development of a Database for Hazard Analyses and Risk Studies. *Natural Hazards Review*. 8(2). DOI: [doi.org/10.1061/\(ASCE\)1527-6988\(2007\)8:2\(23\)](https://doi.org/10.1061/(ASCE)1527-6988(2007)8:2(23))
- [Long-term changes..., 2001](#) – Long-term changes and cyclical fluctuations in the climate of Tbilisi. 2001. Tbilisi, Tr. Institute of Hydrometeorology of Georgia, v. 103. 165 p.

Malmstadt et al., 2010 – Malmstadt, Jill C., Elsner, James, B., Jagger, Th.H. (2010). Risk of Strong Hurricane Winds to Florida Cities. *Journal of Applied Meteorology and Climatology*. 49(10): 2121-2132. DOI: doi.org/10.1175/2010JAMC2420.1

McVicar et al., 2008 – McVicar, T.R., Van Niel, T.G., Li, L.T., Roderick, M.L., Rayner, D.P., Ricciardulli, L., Donohue, R.J. (2008). Wind speed climatology and trends for Australia, 1975–2006: Capturing the stilling phenomenon and comparison with near-surface reanalysis output. *Geophysical Research Letters*. 35: L20403. DOI: 10.1029/2008GL035627

Varazanashvili et al., 2022 – Varazanashvili, O.Sh., Gaprindashvili, G.M., Elizbarashvili, E.Sh., Basilashvili, T.Z., Amiranashvili, A.G. (2022). Principles of Natural Hazards Catalogs Compiling and Magnitude Classification. *Physics of Solid Earth, Atmosphere, Ocean and Space Plasma. Journals of Georgian Geophysical Society*. 25(1): 5-12. DOI: https://doi.org/10.48614/ggs2520224794

Varazanashvili et al., 2023 – Varazanashvili, O., Gaprindashvili, G., Elizbarashvili, E., Basilashvili, Ts., Amiranashvili, A., Fuchs, S. (2023). The First Natural Hazard Event Database for the Republic of Georgia (GeNHs). Catalog. 270 p. [Electronic resource]. URL: http://dspace.gela.org.ge/handle/123456789/10369 DOI: 10.13140/RG.2.2.12474.57286

Varazanashvili et al., 2012 – Varazanashvili, O., Tsereteli, N., Amiranashvili, A., Tsereteli, E., Elizbarashvili, E., Dolidze, J., Qaldani, L., Saluqvadze, M., Adamia, S., Arevadze, N., Gventcadze, A. (2012). Vulnerability, hazards and multiple risk assessment for Georgia. *Natural Hazards Journal of the International Society for the Prevention and Mitigation of Natural Hazards*. 64: 2021-2056. DOI 10.1007/s11069-012-0374-3

Vickery et al., 2000 – Vickery, P.J., Skerlj, P.F., Steckley, A.C., Twisdale, L.A. (2000). Hurricane Wind Field Model for Use in Hurricane Simulations. *Journal of Structural Engineering*. 126(10). DOI: doi.org/10.1061/(ASCE)0733-9445(2000)126:10(1203)

Xie et al., 2006 – Xie L., Bao, Sh., Pietrafesa, L.J., Foley, K., Fuentes, M. (2006). A Real-Time Hurricane Surface Wind Forecasting Model: Formulation and Verification. *Monthly Weather Review*. 134(5). 1355-1370. DOI: doi.org/10.1175/MWR3126.1

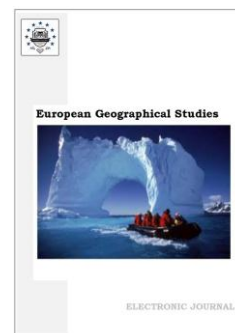
Xu et al., 2006 – Xu, M., Chang, C., Fu, C., Qi, Y., Robock, A., Robinson, D., Zhang, H. (2006). Steady decline of East Asian monsoon winds, 1969–2000: evidence from direct ground measurements of wind speed. *Journal of Geophysical Research-Atmospheres*. 111: D2411. DOI: 10.1029/2006JD007337

Copyright © 2023 by Cherkas Global University



Published in the USA
 European Geographical Studies
 Issued since 2013.
 E-ISSN: 2413-7197
 2023. 10(1): 19-27

DOI: 10.13187/egs.2023.1.19
<https://egs.cherkasgu.press>



Variations in the Tropopause Temperature and Height over the Vu Gia-Thu Bon River Basin in Vietnam: Insights from GNSS Radio Occultation Observations

Thi Hoai Thu Trinh ^{a,*}, Quang Van Nguyen ^a

^a Hanoi University of Natural Resources and Environment, Vietnam

Abstract

This study presents a comprehensive analysis of the tropopause height and temperature over the Vu Gia-Thu Bon river basin using multi GNSS-RO (Global Navigation Satellite System Radio Occultation) data. The findings reveal an average tropopause temperature and height are 195.341K (± 0.166 K) and 16.467 km (± 0.079 km), respectively. Monthly fluctuations in tropopause altitude range from 15.898 km (min) in July 2008 to 17.208 km (max) in February 2010. The highest temperatures and lowest altitudes occur from May to September, while the lowest temperatures and highest altitudes are observed from October to April. Tropopause height varies from 15.848 km to 17.208 km, with deviations from the mean ranging from -0.079 km to 0.232 km. Tropopause temperature ranges from 192.647K to 197.797K, with deviations from the mean ranging from -0.166K to 1.893K. The multi-regression analysis shows a significant upward trend in both tropopause temperature and height from 2002 to 2017. The Tropopause temperature increases approximately by +0.2K with an average yearly increase of 0.013K, while the tropopause height shows an upward trend of about +0.1km with an average yearly increase of 0.008km. The annual and semi-annual periods display sinusoidal variations in both temperature and height, with the annual cycle showing a larger amplitude. These findings highlight the impact of global temperature change on troposphere dynamics, emphasizing the importance of monitoring and understanding these changes for climate forecasting in the Vu Gia-Thu Bon river basin.

Keywords: GNSS-RO, tropopause temperature, tropopause height, trend, Vu Gia-Thu Bon.

1. Introduction

The tropopause, which separates the troposphere and stratosphere, plays a crucial role in atmospheric dynamics. Variations in tropopause temperature and height have important implications. Deep convection in the troposphere plays a key role in transporting mass, heat, and moisture vertically, impacting the temperature and humidity profiles of the tropopause (Reilinger et al., 2006). Changes in convective activity can affect the exchange of water vapor, trace chemicals, and energy between these atmospheric layers. The tropopause acts as a gateway for this exchange, and its height and structure influence the Brewer-Dobson circulation, which affects the distribution of chemical components in the stratosphere (Fueglistaler et al., 2009; Reilinger et al., 2006). Alterations in the tropopause characteristics, such as its height and temperature, are associated with climate change. Human activities, including carbon dioxide emissions and stratospheric ozone depletion, contribute to changes in troposphere and stratosphere dynamics, thereby affecting tropopause features (Lorenz, DeWeaver, 2007; Santer et al., 2004). Given the tropopause's

* Corresponding author
 E-mail addresses: tththu@hunre.edu.vn (T.H. Thu Trinh)

significance in climate dynamics and its response to external factors, continuous monitoring and evaluation of its temperature and height are necessary.

Traditionally, atmospheric profiling has relied on radiosonde observations and reanalysis data. Reanalysis data provides consistent and global coverage but lacks real-time observation capability (Sterl, 2004). Radiosonde observations, on the other hand, offer precise in-situ measurements of temperature, wind, and air pressure with excellent vertical resolution (Wang et al., 2012). However, in regions like Vietnam, specifically in the Vu Gia-Thu Bon River basin, there are challenges regarding the availability and distribution of radiosonde observations in terms of space and time. To overcome these limitations, it is necessary to explore the potential of the Global Navigation Satellite System – Radio Occultation (GNSS-RO) technique. This technique provides improved spatial and temporal resolution, addressing the need for more detailed and frequent observations in the area.

The GNSS-RO technique operates by capturing signals from Global Navigation Satellite Systems (GNSS) in low-Earth orbit (LEO) as they traverse the Earth's atmosphere. Occultation events occur when the LEO satellite receiver becomes obscured or emerges from behind the Earth's surface from the perspective of a GNSS satellite. These events cause the GNSS signal to undergo bending as it propagates through the atmosphere, with its trajectory influenced by atmospheric properties such as pressure, temperature, and water vapor content. The degree of bending is directly linked to the atmospheric parameters. Through the analysis of GNSS signal characteristics during occultation, valuable information regarding atmospheric conditions, including temperature, humidity, and pressure profiles, can be derived using the GNSS-RO technique (Awange, Grafarend, 2005).

The GNSS-RO method offers several advantages that address the limitations associated with conventional observation techniques. It facilitates global coverage, enabling observations to be conducted in remote and inaccessible areas. With its high vertical resolution, the technique enables detailed profiling of the atmosphere. Moreover, GNSS-RO data exhibits long-term stability, making it well-suited for monitoring gradual changes in atmospheric conditions. Notably, the GNSS-RO approach focuses on the critical region of the atmosphere spanning from 7 to 25 kilometers, which corresponds closely to the troposphere's height range. Therefore, GNSS-RO emerges as a valuable tool for monitoring convection processes and obtaining precise measurements of tropopause height and temperature. There have been several studies that have utilized GNSS-RO data to determine tropopause temperature and height at different scales, ranging from global to regional analyses (Awange et al., 2011; Khandu et al., 2016; Nascimento et al., 2020; Schmidt et al., 2005; Schmidt et al., 2008). However, it appears that no specific studies have been conducted for the Vu Gia-Thu Bon river basin using GNSS-RO data.

To obtain tropopause temperature and height information for the Vu Gia Thu Bon river basin using GNSS-RO data, it is crucial to conduct further research or specific studies focusing on this region. The primary objective of this study is to provide valuable insights into the tropopause characteristics and dynamics specific to the Vu Gia-Thu Bon river basin using GNSS-RO data. By analyzing the GNSS-RO data in this particular area, the study aims to enhance our understanding of the local atmospheric processes, including the behavior of the tropopause.

This research endeavor will contribute to filling the existing knowledge gap and facilitating a more comprehensive understanding of the atmospheric conditions in the Vu Gia-Thu Bon river basin from 2002–2017. The findings and insights gained from this study will be instrumental in improving the modeling and prediction of local climate dynamics. Ultimately, the research outcomes will aid in better understanding the interactions between the troposphere and stratosphere, the exchange of mass and energy, and the impact of these processes on the local climate system.

2. Research area and data

Vu Gia-Thu Bon is one of the nine largest basins in Vietnam, located at 14°57'10" to 16°16'50" North latitude, 107°53'50" to 108°12'20" East longitude. In this study, data from multiple occultation missions have been utilized for analysis of the tropopause height and temperature over the Vu Gia-Thu Bon river basin from January 2008 to December 2017. These missions include Challenging Minisatellite Payload (CHAMP), NASA's Gravity Recovery and Climate Experiment (GRACE), the European Meteorological Satellite Organization's Meteorological Operational

Satellite Program (MetOp), and the Constellation Observing System for Meteorology, Ionosphere, and Climate (COSMIC).

The CHAMP mission, which was active from 2001 to 2008, provided valuable data for this analysis. NASA's GRACE mission, which operated from 2007 to 2016, primarily focused on monitoring Earth's gravity field but also contributed to atmospheric research through GNSS-RO measurements. The MetOp satellites, part of the European Meteorological Satellite Organization's Meteorological Operational Satellite Program, have been in operation since 2006 and were specifically designed for weather and climate-related observations. The COSMIC mission, a joint effort between the United States and Taiwan, has been providing high-quality atmospheric, ionospheric, and climate observations since its launch in 2006. By leveraging data from these missions, this study conducts a comprehensive analysis of the tropopause dynamics in the Vu Gia-Thu Bon river basin and investigates its relationship to regional warming patterns.

By combining data from these different occultation missions, the study aims to maximize the availability of observations and enhance the coverage and accuracy of the derived tropopause parameters in the study area.

The dry temperature and tropopause height in this region was extracted from ROM SAF (Radio Occultation Meteorology Satellite Application Facility) central via the link: <https://www.romsaf.org/> (EUMETSAT).

3. Method

3.1 From bending angle dry temperature

GNSS-RO is a satellite remote sensing technology that utilizes GNSS data collected by LEO satellites to profile the Earth's atmosphere. The signals transmitted by the GNSS satellites experience delays in phase and amplitude as they pass through the atmosphere, which can be observed and measured by the LEO satellite.

The phase delay of the GNSS signal is particularly important in GNSS-RO. It is inverted using a mathematical technique called the Abel transformation to derive the refractivity of the air along the signal path. Refractivity is a measure of how much the path of the signal is bent by the atmosphere due to variations in temperature, pressure, and humidity.

During an occultation event, which takes place when a low-Earth orbit (LEO) satellite passes behind or emerges from the Earth's limb from the perspective of a GNSS satellite, the paths of GNSS signals undergo bending as a result of refractivity gradients in the atmosphere. The bending of these signals is depicted in Figure 1, which illustrates the geometry of the GNSS-RO technique. Through the analysis of this signal bending, valuable data pertaining to atmospheric properties along the signal path, including temperature and humidity, can be retrieved.

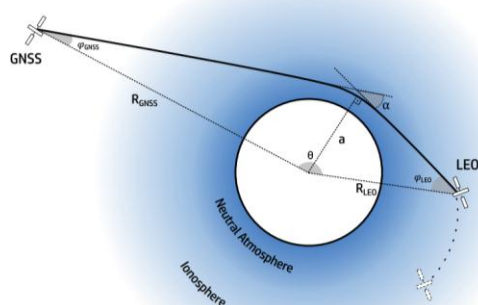


Fig. 1. Geometry of GNSS – LEO satellite occultation

Source: Sievert, 2019

The relationship between the bending angle α , the impact parameter a , and the refractive index n can be described as follows (Awange, Grafarend, 2005):

$$\alpha(a) = -2a \int_{r=r_o}^{r=\infty} \frac{1}{\sqrt{n^2 r^2 - a^2}} \frac{d\{\ln(n)\}}{dr} dr \quad (1)$$

where α represents the bending angle of the signal, a is the impact parameter (the radial distance at the beginning and end of the signal's bending), n is the refractive index, and r the signal's path length.

The inverse Abel transformation is applied to the right-hand side of equation (1) to describe and analyze the associated parameter. This transformation allows for the retrieval of the bending angle, which is obtained from GNSS and LEO satellite location and velocity data, as a function of parameter a . Subsequently, the refractive index n can be calculated based on this relationship, as demonstrated by (Awange, Grafarend, 2005).

$$n(r_o) = \exp \left[\frac{1}{\pi} \int_{a=a_o}^{a=\infty} \frac{\alpha(a)}{\sqrt{a^2 - a_o^2}} da \right] \quad (2)$$

where r_o represents the radius measured from the center of the Earth to the specific height being considered.

In the context of atmospheric science, the relationship between refractivity (N) and refractive index (n) can be expressed:

$$N = (n - 1) * 10^6 \quad (3)$$

This equation relates the refractivity (N) to the refractive index (n) by subtracting 1 from the refractive index and multiplying the result by 10^6 . The refractivity is typically measured in N-units.

The temperature, pressure, and air density can be calculated using the refractivity N through equation 4 (Awange, Grafarend, 2005).

$$N = 77.6 \frac{P}{T} + \left(3.73 \times 10^5 \frac{P_w}{T^2} \right) - \left(40.3 \times 10^6 \frac{n_e}{f^2} \right) + 1.4w \quad (4)$$

where P is the air pressure in mbar, T is the air temperature in K, P_w is the water vapour partial pressure in mbar, n_e is the electron density per cubic meter in number of electrons/m³, f is the transmitter frequency in Hz, and w is the liquid water content in g/m³.

3.2. From dry temperature to tropopause height

The determination of the tropopause position can vary depending on the definition used. The lapse rate tropopause is commonly employed for assessing climatological variability. In this study, the tropopause heights and temperatures were extracted from GNSS RO profiles based on the thermal definition provided by the World Meteorological Organization (WMO) in 1957.

According to the WMO, the tropopause is defined as the lowest level at which the lapse rate (the rate of temperature decrease with height) decreases to 2 degrees Celsius per kilometer (2°C/km) or less. Additionally, it is required that the average lapse rate between this level (referred to as "z") and all higher levels within 2 kilometers above (z + 2) does not exceed 2°C/km. It is important to note that only the first occurrence of the lapse rate tropopause is considered in this study.

The lapse rate (z_i) is determined using expression 5 (Schmidt et al., 2005):

$$\Gamma_{(z_i)} = -\frac{\partial T}{\partial z} = \frac{T_{i+1} - T_i}{z_{i+1} - z_i} \quad (5)$$

where T and z are the temperatures and heights above mean sea level, respectively.

According to WMO definition, when the lapse rate is greater than -2K/km, the following conditions are considered:

- Mean Lapse Rate Condition: The mean lapse rate between the height level z_i and the level $z_i + 2$ km should be larger than -2K/km.

- Layer Comparison Condition: If the mean lapse rate between the layers (z_{i+1}, z_i), (z_{i+2}, z_{i+1}) and (z_{i+3}, z_{i+2}) is greater than -2K/km, and the mean lapse rate between the (z_{i+1}, z_i), (z_{i+2}, z_{i+1}) and (z_{i+3}, z_{i+2}) is less than -2K/km, then it satisfies the condition.

If both of the conditions mentioned earlier are fulfilled, indicating that the lapse rate meets the specified criteria, the lapse rate (z_i) corresponding to that specific lapse rate can be chosen as the lapse rate tropopause.

3.3. From dry temperature and tropopause height to tropopause temperature

In addition to determining the lapse rate tropopause, the temperature at the tropopause can be estimated using linear regression analysis with the dry temperature data corresponding to the selected lapse rate tropopause height. The linear regression model allows for the estimation of temperature values at the tropopause level based on the relationship between the lapse rate tropopause height and the corresponding dry temperature observations. This provides a means to obtain an estimate of the temperature at the tropopause, which is an important parameter for understanding the characteristics and dynamics of the atmosphere in that region.

4. Results and discussion

4.1. Monthly and annual tropopause heights and temperatures

In this study, the tropopause heights and temperatures over the Vu Gia – Thu Bon region have been analyzed on a monthly and annual basis to investigate any variations between these periods. Figure 2 illustrates the monthly mean tropopause heights, while Figure 3 displays the corresponding monthly mean tropopause temperatures. The data used for these analyses were obtained from CHAMP, GRACE, MetOp, and COSMIC missions.

Based on the data analysis, the study reveals that the mean tropopause height over Vu Gia – Thu Bon is estimated to be 16.467 km. Concurrently, the corresponding mean tropopause temperature is found to be 195.341K.

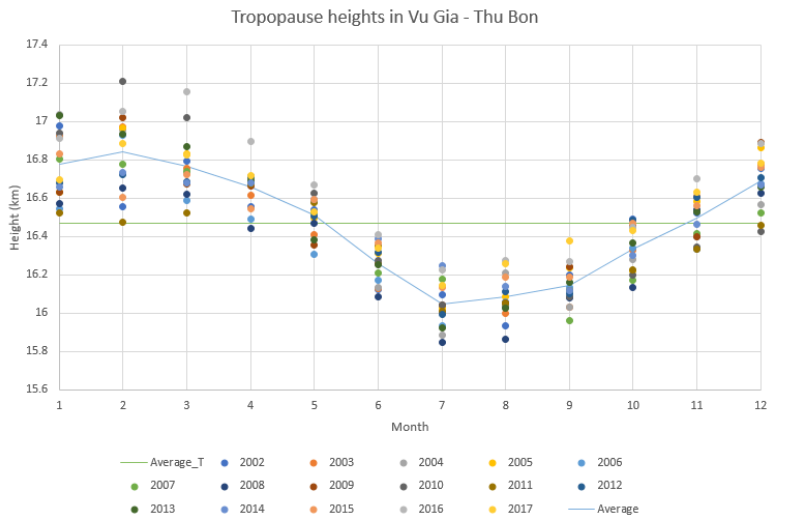


Fig. 2. Tropopause heights in Vu Gia – Thu Bon

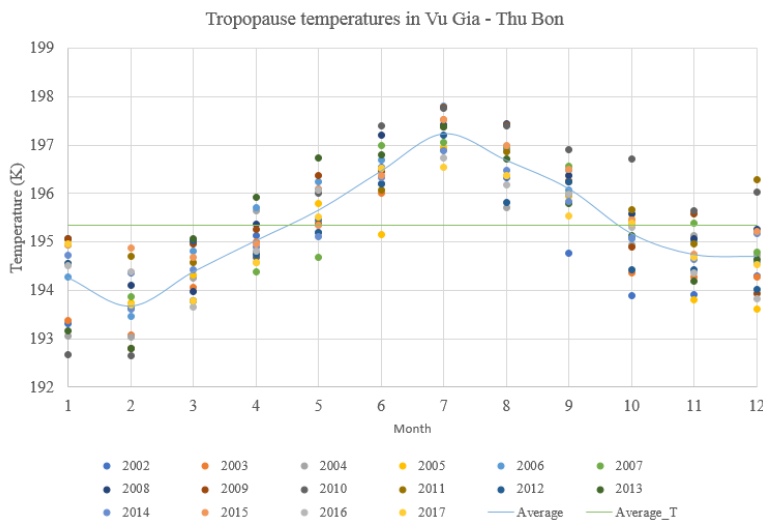


Fig. 3. Tropopause temperatures in Vu Gia – Thu Bon basin

Based on the data presented in Figure 2 and Figure 3, the tropopause altitude in the Vu Gia – Thu Bon region reached its lowest value of 15.898 km in July 2008, while the highest altitude of 17.208 km was recorded in February 2010, coinciding with the highest temperature of 197.797K observed in July 2006 and the lowest temperature of 192.647K in February 2010. These findings demonstrate that the tropopause elevation fluctuates on a monthly basis, with certain months surpassing the average value of 16.467 km. Specifically, in January, February, March, May, November, and December, the altitude exceeds the mean, while in June, July, August, September, and October, the values are lower than the average. Contrasting with the altitude pattern, the tropopause temperature exhibits different trends. Months such as May, June, August, September, and October experience temperatures above the average of 195.341K, while January, February, April, and the months of October, November, and December exhibit temperatures below the mean.

4.2. Seasonal variations

The convective zone in the averaged region exhibits the following patterns: (1) The season with the highest temperature and lowest altitude occurs from May to September, which corresponds to the months when the monitoring station records the highest air temperatures; (2) The season with the lowest temperature and highest altitude is observed from October of the previous year to April of the following year, aligning with the months when the monitoring stations measure lower temperatures; and (3) The tropopause height varies between 15.848 km and 17.208 km across different seasons, with differences from the mean ranging from -0.079 km to 0.232 km. Similarly, the tropopause temperature ranges from 192.647K to 197.797K, depending on the season, with differences from the mean ranging from -0.166K to 1,893K.

4.3. Trend, annual and semianual amplitude analysis

To assess the trend of tropopause temperature and altitude in the Vu Gia-Thu Bon River basin, an analysis is conducted. This analysis includes the examination of level, trends, annual and semiannual cycles of tropopause temperature and altitude, as depicted in Figure 4, 5, and Table 1.

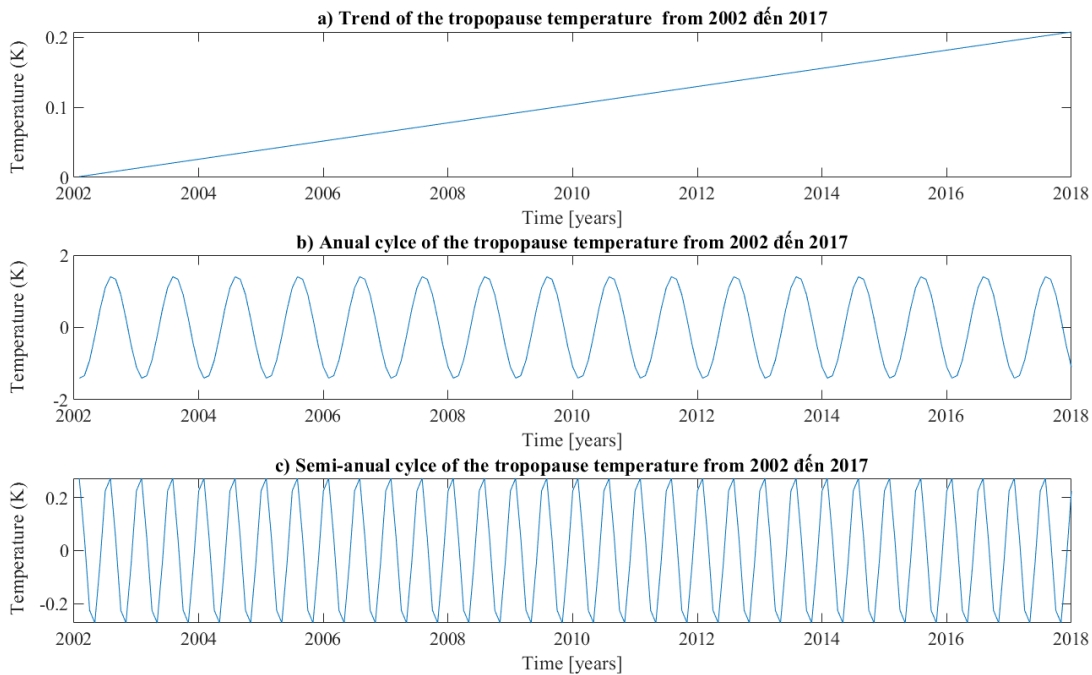


Fig. 4. The trends, annual and semi-annual cycles of the tropopause temperature during the period from 2002 to 2017

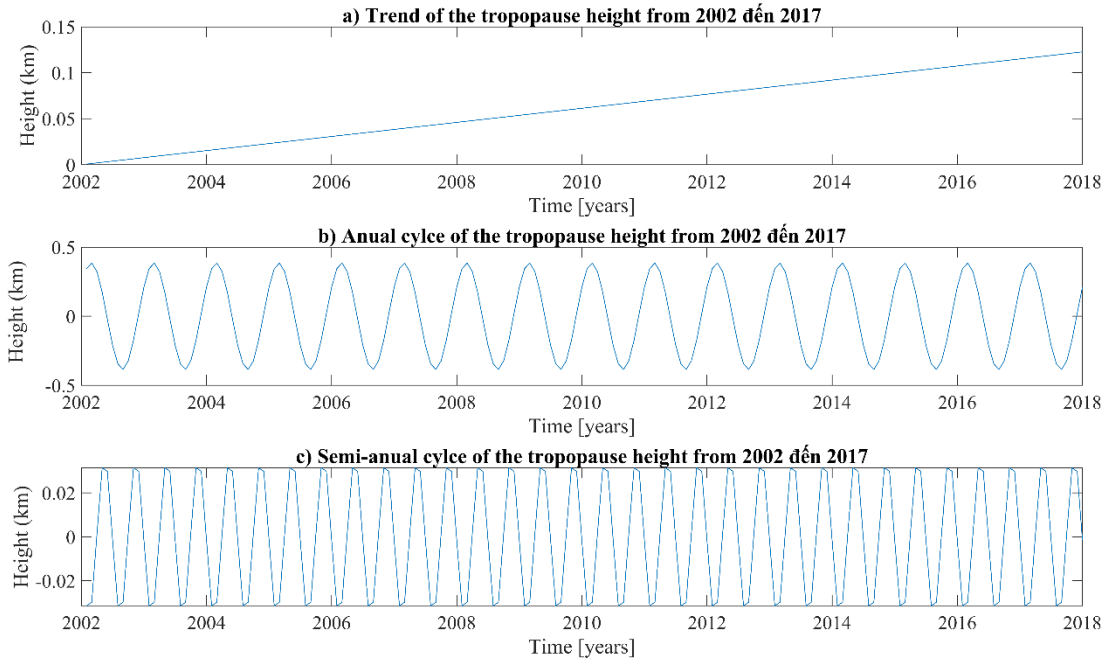


Fig. 5. The trends, annual and semi-annual cycles of the tropopause height during the period from 2002 to 2017

The levels, trends, annual and semi-annual cycles of the tropopause temperature and height were determined using multi-regression analysis. The "level" represents the baseline or average temperature and height of the tropopause during the analyzed period. The "trend" indicates the overall direction and magnitude of the temperature and height change observed over time. The "annual cycle" captures the yearly variations in tropopause temperature and height, reflecting any recurring patterns or seasonal changes. The "semi-annual cycle" highlights the shorter-term variations within each year, displaying the temperature and height fluctuations over a six-month period.

Based on the analysis presented in Figure 4, 5, and Table 1, it can be observed that between 2002 and 2017, both the temperature and height of the tropopause exhibit an upward trend. The tropopause temperature tends to increase by approximately +0.2K during this period, with an average yearly increase of 0.013K. Similarly, the tropopause height shows an upward trend of about +0.1km, with an average yearly increase of 0.008km. These findings provide valuable insights into the long-term changes and variations in tropopause temperature over the specified time frame.

Table 1. The results obtained from determining the levels, trends, and annual and semi-annual cycles for the period 2002–2017

| Properties | Temperature (K) | Altitude (km) |
|---------------------------------------|-----------------|---------------|
| Level | 195.237 | 16.405 |
| Trend/year | 0.013 | 0.008 |
| Annual Amplitude | 1.423 | 0.386 |
| Semi-Annual Amplitude | 0.291 | 0.035 |
| Regression mean square error (RMSE) | 0.620 | 0.129 |
| Regression coefficient R ² | 0.742 | 0.820 |

The tropopause temperature and height exhibit sinusoidal variations in both the annual and semi-annual periods. The annual cycle is the main variation, with a larger amplitude compared with the semi-annual cycle.

5. Conclusion

This study analyzes the tropopause height and temperature over the Vu Gia-Thu Bon River basin using multi GNSS RO (Global Navigation Satellite System Radio Occultation) data in period 2002–2017. The analysis provides valuable insights into the behavior of the tropopause in this region with the following key findings:

1. The average tropopause height was estimated to be 16.467 km, with an average temperature of 195.341K. The tropopause altitude exhibited monthly fluctuations, reaching its lowest point in July 2008 at 15.898 km, and its highest point in February 2010 at 17.208 km.

2. The highest temperatures and lowest altitudes of the tropopause occurred from May to September, while the lowest temperatures and highest altitudes were observed from October to April. The tropopause height ranged from 15.848 km to 17.208 km, with deviations from the mean ranging from -0.079 km to 0.232 km. Similarly, the tropopause temperature ranged from 192.647K to 197.797K, with deviations from the mean ranging from -0.166K to 1.893K.

3. Utilizing multi-regression analysis, the study identified an upward trend in both tropopause temperature and height between 2002 and 2017. The tropopause temperature exhibited an approximate increase of +0.2K with an average yearly increase of 0.013K, while the tropopause height showed an upward trend of about +0.1km with an average yearly increase of 0.008 km. Both tropopause temperature and height displayed sinusoidal variations in the annual and semi-annual periods, with the annual cycle exhibiting a larger amplitude.

The study underscores the impact of global temperature change on tropopause temperature and height. These findings suggest that monitoring changes in tropopause temperature and height can provide valuable insights into regional warming.

6. Acknowledgments

The article received support from the project titled "Determining the relationship between tropopause heights and temperatures with total surface water using GNSS satellite data and remote sensing data" [grant numbers: TNMT.2021.02.04].

References

- Awange, Grafarend, 2005 – Awange, J.L., Grafarend, E.W. (2005). GPS meteorology in environmental monitoring. *Solving Algebraic Computational Problems in Geodesy and Geoinformatics: The Answer to Modern Challenges*, 217-244.
- Awange et al., 2011 – Awange, J., Wickert, J., Schmidt, T., Sharifi, M., Heck, B., Fleming, K. (2011). GNSS remote sensing of the Australian tropopause. *Climatic Change*. 105: 597-618.
- EUMETSAT – EUMETSAT [Electronic resource]. URL: <https://www.romsaf.org/>
- Fueglistaler et al., 2009 – Fueglistaler, S., Dessler, A., Dunkerton, T., Folkins, I., Fu, Q., Mote, P.W. (2009). Tropical tropopause layer. *Reviews of Geophysics*. 47(1).
- Khandu et al., 2016 – Khandu, K., Awange, J., Forootan, E. (2016). Interannual variability of temperature in the UTLS region over Ganges–Brahmaputra–Meghna river basin based on COSMIC GNSS RO data. *Atmospheric Measurement Techniques*. 9: 1685-1699.
- Lorenz, DeWeaver, 2007 – Lorenz, D.J., DeWeaver, E.T. (2007). Tropopause height and zonal wind response to global warming in the IPCC scenario integrations. *Journal of Geophysical Research: Atmospheres*. 112(D10).
- Nascimento et al., 2020 – Nascimento, A., Awange, J., Gonçalves, R. (2020). South America's tropopause variability in relation to global teleconnection (2001–2017): A GNSS-radio occultation assessment. *Journal of Atmospheric and solar-terrestrial physics*. 209: 105379.
- Reilinger et al., 2006 – Reilinger, R., McClusky, S., Vernant, P., Lawrence, S., Ergintav, S., Cakmak, R., ... Stepanyan, R. (2006). GPS constraints on continental deformation in the Africa-Arabia-Eurasia continental collision zone and implications for the dynamics of plate interactions. *Journal of Geophysical Research: Solid Earth*. 111(B5).
- Santer et al., 2004 – Santer, B., Wehner, M., Wigley, T., Sausen, R., Meehl, G., Taylor, K., ... Boyle, J. (2004). Response to Comment on "Contributions of anthropogenic and natural forcing to recent tropopause height changes". *Science*. 303(5665): 1771-1771.

[Schmidt et al., 2005](#) – Schmidt, T., Heise, S., Wickert, J., Beyerle, G., Reigber, C. (2005). GPS radio occultation with CHAMP and SAC-C: global monitoring of thermal tropopause parameters. *Atmospheric Chemistry and Physics*. 5(6): 1473-1488.

[Schmidt et al., 2008](#) – Schmidt, T., Wickert, J., Beyerle, G., Heise, S. (2008). Global tropopause height trends estimated from GPS radio occultation data. *Geophysical Research Letters*. 35(11).

[Sievert, 2019](#) – Sievert, T. (2019). GNSS Radio Occultation Inversion Methods and Reflection Observations in the Lower Troposphere. Blekinge Tekniska Högskola.

[Sterl, 2004](#) – Sterl, A. (2004). On the (in) homogeneity of reanalysis products. *Journal of Climate*. 17(19): 3866-3873.

[Wang et al., 2012](#) – Wang, J. S., Seidel, D. J., Free, M. (2012). How well do we know recent climate trends at the tropical tropopause? *Journal of Geophysical Research: Atmospheres*. 117(D9).